High Frequency (139.5 GHz) Electron Paramagnetic Resonance Spectroscopy of the GTP Form of p21 *ras* with Selective ^{17}O Labeling of Threonine†

Christopher J. Halkides,‡,§ Brendan F. Bellew,|| Gary J. Gerfen,|| Christian T. Farrar,|| Percy H. Carter,⊥ Bernice Ruo,⊥ David A. Evans,⊥ Robert G. Griffin,*,|| and David J. Singel*,#

Department of Biochemistry, Brandeis University, Waltham, Massachusetts 02154, Department of Chemistry and Francis Bitter Magnet Laboratory, Massachusetts Institute of Technology, Cambridge, Massachusetts 02139, Department of Chemistry, Harvard University, Cambridge, Massachusetts 02138, and Department of Chemistry and Biochemistry, Montana State University, Bozeman, Montana 59717

Received March 11, 1996; Revised Manuscript Received July 9, 1996⊗

ABSTRACT: Electron paramagnetic resonance spectroscopy at 139.5 GHz has been used to study p21 *ras* complexed with Mn(II) and guanosine 5′-(β,γ-imidotriphosphate), an analog of GTP. The p21 sample studied was selectively labeled with [$^{17}O_\gamma$]threonine to a final enrichment of 30%. A Mn(II)−^{17}O hyperfine interaction was observed, but the value of the coupling constant, 0.11 ± 0.04 mT, is the smallest such value yet reported. *Ab initio* calculations indicate that this value is consistent with direct coordination of the threonine hydroxyl group and provide an estimate for the Mn(II)−^{17}O bond length of 2.7 Å. The measured hyperfine coupling constant and associated bond length starkly contrast with typical values for Mn(II)−^{17}O coordination complexes, namely, ∼0.25 mT and ∼2.2 Å, respectively. This contrast underscores the peculiar weakness of this Mn(II)−O interaction in p21 and persuasively argues that the nucleotide-induced conformational change, which is known to encompass the region of p21 involving Thr35, is not driven by Mn(II) coordination of the Thr35 hydroxyl group.

The *ras* gene product, p21,[1] belongs to the family of homologous GTP-hydrolyzing proteins and plays a major role in cell signal transduction (Bourne *et al.*, 1990). The active and inactive forms of p21 bind the metal complexes of GTP and GDP, respectively (Milburn *et al.*, 1990). Auxiliary proteins catalyze the interconversion between the two states, as discussed in the preceding paper (Bellew *et al.*, 1996).

X-ray diffraction studies of p21 in the two nucleotide forms have delineated two regions of conformational changes: the first encompasses residues 32−40 and the second residues 60−76 (Milburn *et al.*, 1990; Pai *et al.*, 1990). While not agreeing on all points, both crystallographic studies showed that Thr35 was coordinated *via* its hydroxyl group to the divalent metal in the GTP form but not the GDP form. Significantly, it has been asserted that the coordination of Thr35 is a cause of the pivotal conformational change in p21 involving residues 32−40 (Marshall, 1993; Milburn *et al.*, 1990; Pai *et al.*, 1990). In qualitative agreement with crystallographic work, ESEEM studies of p21·Mn(II)·GMPPNP in solution also show that Thr35 is closer in the GTP than in the GDP state; however, ESEEM places Thr35 further away from the divalent metal ion in the GTP form than does X-ray crystallography (Halkides *et al.*, 1994).

In order to determine the distance between the divalent cation and Thr35 in the absence of interprotein contacts that might perturb the molecular structure in the crystal, ESEEM studies were carried out on frozen solutions of p21 selectively labeled with [^{15}N]Thr, [3-^{2}H]Thr, and [3-^{13}C]Thr, and with Mn(II) as the divalent cation. These measurements showed that the distance between the manganous ion and the hydroxyl oxygen of Thr35 must be at least 2.8 Å (Halkides *et al.*, 1994). This distance is significantly larger than is typical of first sphere oxygen−manganous ion coordination, ∼2.16−2.20 Å (Bruckner *et al.*, 1993; Carrell *et al.*, 1988; Carrell & Glusker, 1973; Ciunik & Glowiak, 1980; Clegg *et al.*, 1987; Glusker & Carrell, 1973; Karipides & Reed, 1976; Lenstra & Dillon, 1983; Sabat *et al.*, 1985; Vasic *et al.*, 1985). These observations imply either that Thr35 coordinates the manganous ion directly, but weakly, or indirectly with an intervening water molecule, reminiscent of Asp57 in the GDP form of p21 (Halkides *et al.*, 1994). Indeed, these results suggest that the pivotal conformational change might be driven by interactions other than the coordination of the hydroxyl group of Thr35. We have argued that coordination of the hydroxyl group is unlikely

† Supported by NIH Grant GM-38352 (R.G.G. and D.J.S.). C.J.H. was supported by NIH Postdoctoral Fellowship CA-08872. G.J.G. was supported by Postdoctoral Fellowships from NIH (GM-14404) and ACS (PF-3668).

* Authors to whom correspondence should be addressed.

‡ Brandeis University.

§ Present address: Institute of Molecular Biology, University of Oregon, Eugene, OR 97403.

|| Massachusetts Institute of Technology.

⊥ Harvard University.

Montana State University at Bozeman.

⊗ Abstract published in *Advance ACS Abstracts,* August 15, 1996.

[1] Abbreviations: p21, product of the *ras* genes; N, neuroblastoma; H, Harvey; GAP, GTPase-activating protein; GAP334, the catalytic domain of GAP; EF-Tu, elongation factor Tu; EPR, electron paramagnetic resonance; ESEEM, electron spin-echo envelope modulation; EDEPR, echo-detected EPR; *m*/*z*, mass-to-charge ratio; NMR, nuclear magnetic resonance; ENDOR, electron−nuclear double resonance; GDP, guanosine 5′-diphosphate; GTP, guanosine 5′-triphosphate; GMPPNP, guanosine 5′-(β,γ-imidotriphosphate); CI, chemical ionization; FAB, fast atom bombardment; cw, continuous wave; GC/MS, gas chromatography/mass spectrometry; LC, liquid chromatography; NF-1, neurofibromin, the product of the neurofibromatosis type 1 gene; Raf-RBD, the p21 *ras* binding domain of Raf1; Rap1A-p21, the protein product of K*rev*-1.

S0006-2960(96)00595-8 CCC: $12.00

to drive the conformational change on energetic grounds: weak threonine hydroxyl coordination is likely to be a consequence of, rather than a cause of, the larger conformational change (Halkides *et al.*, 1994).

To provide decisive experimental evidence in support of this view, we have undertaken to characterize more fully the interaction between the threonine hydroxyl group and the metal ion of Mn(II)−p21 complexes in solution. Bellew *et al*. (preceding paper) employed continuous wave EPR spectroscopy together with protein preparation in $H_2{}^{17}O$ to determine the number of water molecules coordinating the manganous ion of p21 in the GTP form. Since three nonaquo ligands other than Thr35 are observed to coordinate the divalent cation, a hydration number of three would indicate the presence of an intervening water ligand. A hydration number of two, however, was observed, thus suggesting the absence of an intervening water molecule in the linkage between the manganous ion and the hydroxyl oxygen of Thr35.

To probe the nature of this linkage more directly, we have undertaken a complementary measurement of the [$^{17}O_\gamma$]Thr−Mn(II) hyperfine interaction of the p21·Mn(II)·GMPPNP complex in frozen solution, using high frequency EPR spectroscopy. Although ^{17}O labeling of exogenous ligands has often been employed fruitfully to probe oxygen coordination (Lodato & Reed, 1987), the study reported here is the first applied to an endogenous ligand in a protein incorporating a selectively ^{17}O-labeled amino acid.

As discussed more extensively in the preceding paper (Bellew *et al.*, 1996), the measurement of ^{17}O hyperfine interactions in manganous ion-based systems depends upon the detection of hyperfine broadening from ^{17}O-labeled oxo ligands against a background of other sources of broadening—principally unresolved ^{1}H and ^{31}P hyperfine interactions and second-order fine structure broadening. The contribution of unresolved hyperfine interactions to the overall line broadening is independent of magnetic field strength; the contribution of second-order fine structure broadening is inversely proportional to the external magnetic field strength (Abragam & Bleaney, 1970). Accordingly, EPR of manganous ion-based systems with ^{17}O labeling has been extended to 139.5 GHz in order to determine the number of coordinated $H_2{}^{17}O$ molecules (Bellew *et al*., 1996 (preceding paper)) and, in this work, to determine the magnitude of ^{17}O hyperfine interactions.

Structural details of the Mn(II)−[$^{17}O_\gamma$]Thr coordination in the p21·Mn(II)·GMPPNP complex influence the strength of the [$^{17}O_\gamma$] hyperfine interaction. Here we report the experimental determination of this hyperfine interaction—the smallest yet reported for ^{17}O coordinated to Mn(II), as well as comparisons with *ab initio* calculations on a $Mn(H_2O)_6^{2+}$ model system. These studies, in conjunction with previous ESEEM results on p21·Mn(II)·GMPPNP, are consistent with a [$^{17}O_\gamma$]Thr−Mn(II) bond which is substantially longer than that observed in X-ray diffraction studies. The role of Thr35 in the interactions of *ras* p21 with other proteins is interpreted in light of these results.

MATERIALS AND METHODS

^{17}O-Labeled Threonine. The synthesis of $^{17}O_\gamma$-enriched threonine relied on an Evans asymmetric aldol reaction (Evans *et al.*, 1983) between ^{17}O-enriched acetaldehyde **1** and imide **2** to establish the absolute and relative stereochemistry of the amino acid (Scheme 1). The ^{17}O-enriched acetaldehyde was obtained from ^{17}O-enriched water (Monsanto) *via* a slight modification of the method of Sawyer (1972). Imide **2** has been used previously in the syntheses of several amino acids, including threonine (Evans & Weber, 1986). Reaction of the tin enolate of **2** with **1** proceeded smoothly, affording diastereomerically pure **3** in 53% yield after silica gel chromatography. Conversion of **3** to threonine followed our previous procedure (Weber, 1987). Hydrolysis of **3** provided both the acid **4** and recovered 4-(phenylmethyl)-2-oxazolidinone in quantitative yield. Removal of the thiocarbonate was achieved under acidic conditions, giving the threonine salt **5** as a light tan solid in 98% yield. Trituration of this material with cold tetrahydrofuran afforded the analytically pure hydrochloride salt used in this study.

Scheme 1

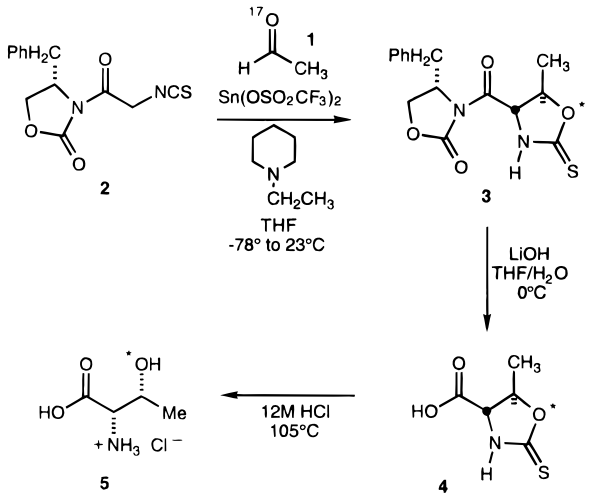

Protein. The H-*ras* gene was cloned from plasmid pXVR (a generous gift of Professor L. Feig) into ptrc99C by standard methodology (C. J. Halkides, unpublished experiments). Overexpression and purification of H-*ras* p21 in the *Escherichia coli* strain DL39TG (auxotrophic for threonine) and the preparation of the p21·Mn(II)·GMPPNP complex in 15% methyl α-D-glucopyranoside were performed as described previously (Halkides *et al.*, 1994; Bellew *et al.*, 1996 (preceding paper)). The activity of p21 was assayed in GAP334-dependent GTPase reactions (Gideon *et al.*, 1992), as described previously (Halkides *et al.*, 1994).

Mass Spectrometry. The enrichment of $^{17}O_\gamma$ in free threonine was determined by introducing 50 μL of a 0.5 mg/mL alcohol/water solution of threonine into a Finnegan 4500 GC/LC/MS directly *via* a moving belt LC/MS interface over 30 s. Isobutane CI was used at 0.5 Torr and 170 °C. A spectrum of unlabeled threonine was also taken, as well as two mixtures of known composition of labeled and unlabeled material. Scans were taken over 60−130 mass units every 5 s. The enrichment of ^{17}O was determined to be 33.8%. To confirm the level of enrichment, a second sample was prepared in a glycerol matrix for FAB using a JEOL SX102A and 6 keV xenon atoms for bombardment. Data were collected by scanning a limited mass range over the appropriate molecular region. The enrichment of ^{17}O was determined to be 33.9%, in excellent agreement with the CI method.

To determine the ^{17}O enrichment of the amino acid residues, in particular threonine, within p21, we hydrolyzed

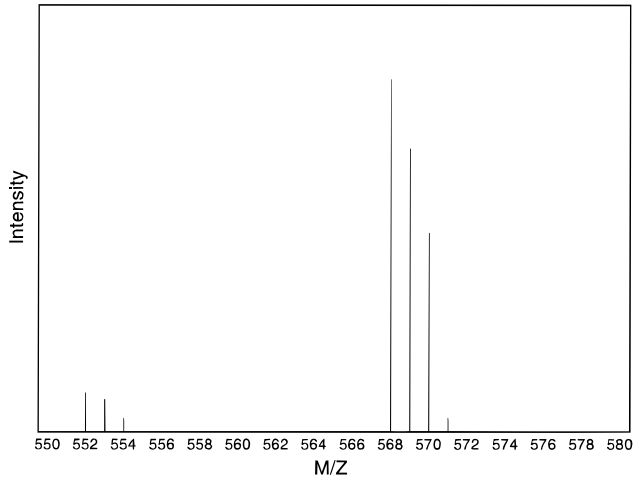

FIGURE 1: A portion of the mass spectrum ($m/z = 550-580$) for the *N*-[(heptafluoro)butyryl]isobutyl derivative of threonine obtained from the hydrolysis of *ras* p21. The hydrolysate was derivatized and subjected to GC and ammonia CI as described under Materials and Methods. The peak at 568 is the parent (molecular) ion (M + 1), in which ^{16}O is present in the hydroxyl group. The peak at 569 arises primarily from the species in which ^{17}O is present in the hydroxyl group, with contributions from natural abundance heavy isotopes elsewhere in the molecular ion. Likewise, the peak at 570 arises primarily from ^{18}O in the hydroxyl group. From these data, we calculate the enrichment of threonine residues labeled with ^{17}O in the protein to be 30.3 ± 0.5%.

a sample of protein and synthesized the *N*-[(heptafluoro)-butyryl] isobutyl esters of the resulting amino acids, as described previously (Halkides *et al.*, 1994). GC/MS on the mixture employed a 30 m by 0.25 mm column of DB5 MSFSCC (J & W Scientific). The injector temperature was 275 °C. The time program was an initial temperature of 80 °C for 2.5 min, followed by an increase of 4 °C/min to 240 °C and held there for 20 min. Compounds were subjected to ammonia CI at 0.7 Torr with an ion source temperature of 170 °C. 70 scans/min ($m/z = 270-700$) were taken. The ^{17}O enrichment of threonine in the protein was determined by analysis of mass spectrometric intensities exhibited by the derivatived protein hydrolysate in the 550−580 range of m/z relevant to threonine precursors (Figure 1). In this analysis we assume natural isotopic abundance for all atoms with the *sole* exception of the threonine γ oxygen (indicated by the * in Scheme 1), and thereby determine a 30.3% relative abundance of [$^{17}O_\gamma$]threonine.

Echo-Detected EPR Spectroscopy. In the preceding paper (Bellew *et al.*, 1996), ^{17}O hyperfine interactions with Mn(II) were determined through the simulation of phase-quadrature detected cw EPR spectra. The same procedure was initially applied in this study and yielded results consistent with an [$^{17}O_\gamma$]Thr35 hyperfine coupling constant of less than 0.15 mT (*vide infra).* Subtle lineshape distortions—deviations from pure absorption lineshapes—related to minor phasing errors (0.005π) impose an undesired limit on precision of this method for determining such small hyperfine coupling constants. In order to eliminate this phasing uncertainty and thus to determine more precisely the [$^{17}O_\gamma$]Thr hyperfine coupling, we employed EDEPR (echo-detected EPR) spectroscopy. By carefully maintaining appropriately small nutation angles, this technique produces spectra analogous to integrated modulation-detetected cw absorption signals without the need for phase correction schemes.

The pulsed 139.5 GHz EPR spectrometer is described in detail elsewhere (Becerra *et al.*, 1995). The external magnetic field was swept through the lowest-field member of the ^{55}Mn hyperfine sextet ($M_I = -5/2$) within the central fine structure transition ($M_S = +1/2 \rightleftharpoons -1/2$) (Reed & Markham, 1984), from 4.9513 to 4.9620 T in 0.0250 mT increments. The microwave power at the resonator was approximately 800 μW, which corresponds to a B_1 field of 0.06 mT. The $p_{\pi/2}-\tau-p_\pi$ (Hahn echo) and $p_{\pi/2}-\tau-p_{\pi/2}-\tau-p_{\pi/2}$ (stimulated echo) pulse sequences were employed. The $\pi/2$ pulse width was ∼200 ns, and the time between pulses, τ, was typically 350 ns.[2] The resulting electron spin echo was integrated and averaged 1000 repetitions per datum. A steady flow of cold helium gas over the resonator maintained the sample within ±0.5 K of, typically, 20 K. In order to assess the influence of homogeneous broadening on the observed EPR lineshapes, we measured the characteristic time constant of the Hahn echo envelope decay (the phase memory time) at 14 K (∼910 ns) and at 20 K (∼725 ns). For pairs of samples differing only in [$^{17}O_\gamma$]Thr enrichment, phase memory times were measured to be the same within ∼5%.

ANALYSIS

Hyperfine Coupling Constant. We determine the magnitude of the [$^{17}O_\gamma$]Thr−Mn(II) isotropic hyperfine interaction using a technique similar to that introduced previously (Kalbitzer *et al.*, 1984; Reed & Leyh, 1980) and described in full detail in the preceding paper (Bellew *et al.*, 1996). Spectra obtained from [$^{17}O_\gamma$]Thr-enriched samples, S_e, are compared with a series of simulations generated by variation of the ^{17}O hyperfine coupling constant. As a check to ensure that the hyperfine coupling constants can be determined accurately using spectra with echo-detected as well as modulation-detected lineshapes, we applied the simulated broadening technique to integrated modulation-detected absorption spectra obtained from p21·Mn(II)·GDP and p21·Mn(II)·GMPPNP in $H_2{}^{17}O$. The results obtained were identical to those described in the previous paper. We also applied the technique to pseudo-modulated (Hyde *et al.*, 1992) EDEPR spectra of the [$^{17}O_\gamma$]Thr−Mn(II) sample and obtained results identical to those presented in this study.

As discussed in the previous paper, the small anisotropic component of the ^{17}O hyperfine coupling is not explicitly modeled in these simulations. This is justified by the typically small value of the anisotropic component, which is less than 20% of the isotropic value (Glotfelty, 1978; Tan *et al.*, 1995, 1993). Furthermore, we have confirmed through simulations that its inclusion has a negligible effect on the determination of the isotropic hyperfine coupling. This method was employed in the preceding paper to determine $H_2{}^{17}O$−Mn(II) isotropic hyperfine coupling constants which were found to be in excellent agreement with values obtained by other methods. Moreover, the inclusion of only isotropic coupling in the analysis requires that any spectral broadening

[2] The small amount of power available at the sample (<1 mW), together with signal-to-noise considerations, forced the microwave pulse widths to be on the order of the interpulse delays. Although not ideal for the precise definition of nutation angles and precession times, the low-power/long-pulse experiment is advantageous in this application of echo-detected EPR for the excitation of narrow spectral bandwidths and for the suppression of nuclear modulation effects.

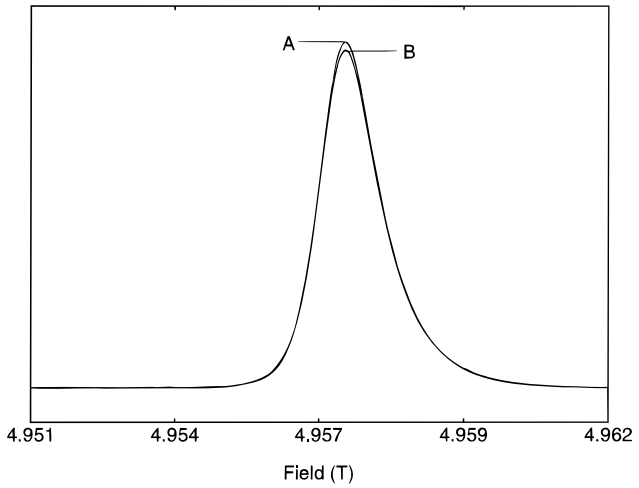

FIGURE 2: Overlying echo-detected EPR signals of *ras* p21·Mn(II)·GMPPNP in frozen solutions at pH 7.3 with 15% methyl α-D-glucopyranoside. (A) Natural abundance [O_γ]Thr, and (B) 30.3 ± 0.5% enriched [$^{17}O_\gamma$]Thr.

resulting from hyperfine anisotropy be accounted for by an increase in the isotropic component. This would tend to favor an overestimate of the isotropic hyperfine coupling constant and subsequently an underestimate of the ^{17}O−Mn(II) bond distance; any distance estimates derived from these measured ^{17}O hyperfine values can be considered as lower bounds. We feel this method is preferable to making assumptions regarding the value of the hyperfine anisotropy, particularly in the present application in which an unusually long ^{17}O−Mn(II) bond is reported.

RESULTS

Experimental Determination of the ^{17}O Hyperfine Coupling. A portion (the low-field line of the ^{55}Mn hyperfine sextet belonging to the $M_S = +1/2 \rightleftharpoons -1/2$ transition) of EDEPR spectra representative of those used to determine the [$^{17}O_\gamma$]Thr hyperfine coupling constant in p21·Mn(II)·GMPPNP are shown in Figure 2. Spectrum A is an experimentally acquired EPR signal of natural abundance p21·Mn(II)·GMPPNP frozen in an aqueous solution of 15% (w/v) methyl α-D-glucopyranoside; spectrum B is the corresponding signal of p21·Mn(II)·GMPPNP with 30.3 ± 0.5% [$^{17}O_\gamma$] enrichment in the threonine residues. For the purpose of quantitative comparison, these spectra are normalized as described in the preceding paper.

Figure 3 illustrates the method by which we estimate the magnitude of the ^{17}O hyperfine coupling constant. Spectra A and B (solid) are the same pair of EPR signals shown in Figure 2. Traces C, D, E, and F (dashed) represent spectrum A after numerical broadening (*vide supra*) by ^{17}O hyperfine coupling constants equal to 0.05, 0.10, 0.15, and 0.20 mT, respectively. The relation of spectrum B to traces D and E shows the actual hyperfine coupling constant is between 0.10 and 0.15 mT. Interpolation yields a value of 0.11 mT as the best estimate of the hyperfine coupling constant.

The dependence of relative peak height upon ^{17}O hyperfine coupling constant is summarized in Figure 4. The curve shows that a relative peak height of 0.976 corresponds to a hyperfine value of 0.11 mT. The slope of the curve in the region of A = 0.10−0.15 mT suggests that a ±1% uncertainty in the relative peak height leads to a 0.03 mT

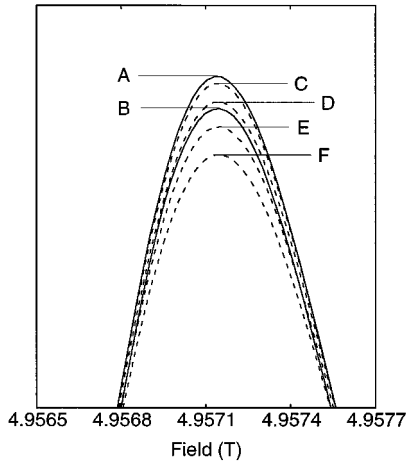

FIGURE 3: The solid traces are EPR signals of *ras* p21·Mn(II)·GMPPNP in frozen solutions as in Figure 2 with (A) natural abundance and (B) 30.3% enriched [$^{17}O_\gamma$]Thr. The dashed traces represent spectrum A after being broadened by a simulated hyperfine interaction with 30.3% enriched [$^{17}O_\gamma$]Thr using an ^{17}O hyperfine coupling constant equal to (C) 0.05, (D) 0.10, (E) 0.15, and (F) 0.20 mT respectively. These data imply that the hyperfine interaction is 0.11 mT.

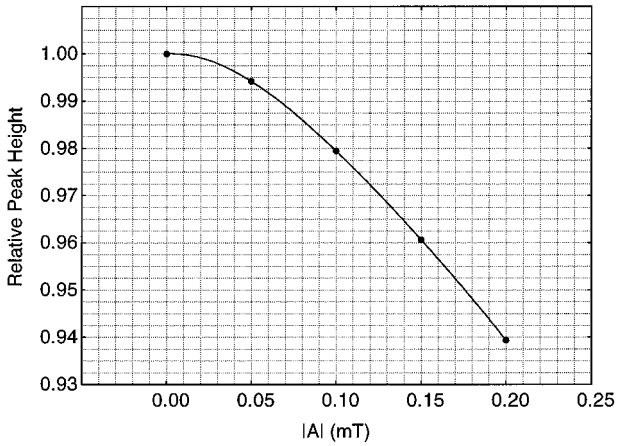

FIGURE 4: Relative peak height of a normalized echo-detected EPR signal for *ras* p21·Mn(II)·GMPPNP with 30.3% enriched [$^{17}O_\gamma$]-Thr. The experimentally acquired EPR signal of *ras* p21·Mn(II)·-GMPPNP with natural abundance [O_γ]Thr is broadened numerically by a computer program which simulates the effects of the ^{17}O hyperfine interaction.

uncertainty in the value of A. Another source of uncertainty in the final estimate of A is uncertainty in the [$^{17}O_\gamma$]Thr enrichment: a ±1% uncertainty in the enrichment leads to a 0.01 mT uncertainty in the value of A. Analysis of several trials yields a [$^{17}O_\gamma$]Thr35 hyperfine coupling of 0.11 +0.03/−0.04 mT in p21·Mn(II)·GMPPNP. This value is substantially smaller than previously observed for a variety of ^{17}O ligands to Mn(II) (Table 1, preceding paper).

Ab Initio Calculations. To gain insight into the implications of this unusually small hyperfine coupling for the Mn(II)−[O_γ]Thr structure, we carried out MO calculations for a model compound, $Mn(H_2O)_6^{2+}$, in various octahedral geometries. *Ab initio* unrestricted Hartree−Fock molecular orbital calculations were performed with the *Gaussian 92* Revision A suite of programs (Frisch *et al.*, 1992). The LANL1MB basis set comprises the STO-3G basis set for first row elements and the Los Alamos ECP + MBS on atoms Na−Bi (Hay & Wadt, 1985a,b; Wadt & Hay, 1985).

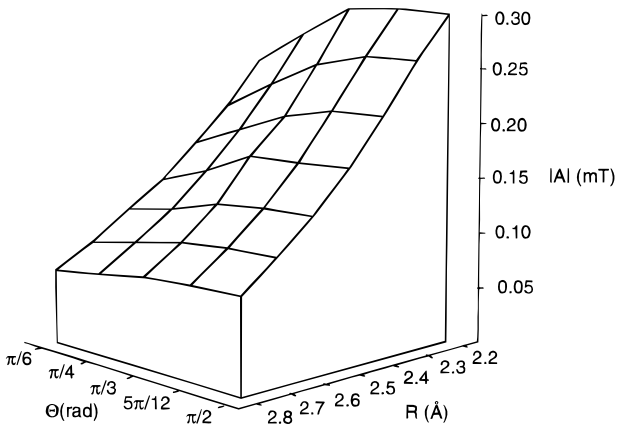

FIGURE 5: Isotropic ^{17}O hyperfine coupling as a function of position and orientation. Couplings are based on Fermi contact analysis of *ab initio* calculations for the model compound $[Mn(H_2O)_6]^{2+}$. R is the Mn−O distance. Θ is the angle between the Mn−O axis and the normal to the H−O−H plane.

We initiated these calculations using the structure of the $Mn(H_2O)_6^{2+}$ guest complex in lanthanum magnesium double nitrate, previously characterized by EPR, ^1H and ^{17}O ENDOR (DeBeer *et al.*, 1973; Glotfelty, 1978). In this structure, the oxygen atoms of the six water ligands surround the central Mn(II) ion in a nearly regular octahedral array with Mn(II)−O bond lengths of 2.20 Å; the angle Θ between the normal to the plane of a water ligand and its Mn−O axis is $\pi/2$. Additional details of the structure of this model complex appear in (DeBeer *et al.*, 1973; Glotfelty, 1978). From a Fermi contact analysis of the results of the MO calculation, we obtained a coupling constant of −8.9 MHz (−0.32 mT) in good agreement with the experimental value of −7.6 MHz (−0.28 mT) (Glotfelty, 1978).

We then applied this computational procedure to explore the effects of metal−ligand structure on the ^{17}O hyperfine coupling. Five of the aquo ligands were maintained at their orientations and the 2.20 Å bond lengths specified above, while the position of the sixth ligand was parametrically varied. We restricted this variation to the physically reasonable geometries in which $\pi/6 \leq \Theta \leq \pi/2$, and we sampled the Mn−O bond lengths from 2.2 to 2.8 Å. Within this neighborhood, calculated values of the ^{17}O hyperfine coupling exhibited little sensitivity to the orientation of the water ligand, but a steep dependence on bond length, as illustrated in Figure 5. Qualitatively, these results clarify the strong correlation of Mn-O bond length with the ^{17}O hyperfine coupling; quantitatively, they suggest that the measured coupling of 0.11 mT indicates a Mn−O bond length of ∼2.7 Å.

DISCUSSION

Structural Implications. In this study, analysis of repeated EDEPR experiments on $[^{17}O_\gamma]$Thr35 in p21·Mn(II)·GMPPNP reveals the $[^{17}O_\gamma]$Thr hyperfine coupling constant to be 0.11 +0.03/−0.04 mT. This coupling is the smallest ^{17}O hyperfine interaction reported for an oxo-ligand in the first coordination sphere of a manganous ion as determined by ENDOR (Glotfelty, 1978; Tan, 1993; Tan *et al.*, 1993), or by EPR (Feuerstein *et al.*, 1987; Kalbitzer *et al.*, 1984; Latwesen *et al.*, 1992; Reed & Leyh, 1980) (Table 1, preceding paper). The existence of an $[^{17}O_\gamma]$Thr35 hyperfine coupling of the same *order of magnitude* as exhibited in more typical Mn(II)−^{17}O complexes establishes that the manganese is directly coordinated by the labeled oxygen, with no intervening water ligand. On the other hand, the relatively small size of the coupling suggests that the manganese−oxygen linkage is unusually weak.

Some insight into the origin of this weakness can be obtained by considering the *variation* among the ^{17}O hyperfine couplings observed for Mn(II) coordinated to various ^{17}O-labeled oxo ligands (Table 1, preceding paper). The couplings observed for $H_2{}^{17}O$ are tightly clustered in the range 0.25−0.28 mT, whereas values for the ^{17}O-labeled ligand atoms in nucleotide polyphosphates span a significantly wider range (0.16−0.4 mT). This distinctive behavior is most readily understood—particularly in light of the MO calculations reported above—as reflecting distinctions in coordination geometries. For small ligands such as H_2O, the metal−ligand structure is determined predominantly, if not exclusively, by the manganese−oxygen interaction itself, whereas for much larger ligands, the adopted structure represents a compromise between the manganese−oxygen interaction and numerous other constraints. An H_2O ligand can thus generally attain a coordination structure that is "optimal" (with respect to the Mn−O interaction alone) and thus exhibit a Mn−O bond length of ∼2.2 Å and a hyperfine coupling of ∼2.5 MHz. By contrast, a phosphoryl oxygen in a nucleotide polyphosphate is subjected to additional constraints by covalent linkages within the nucleotide, by noncovalent interactions between the nucleotide and surrounding protein and, potentially, by the coordination of other phosphate oxygens to the metal center. Accordingly, it may be compelled to adopt a less than "optimal" Mn(II)−O structure. Although such structural perturbations might be small, they can nevertheless lead to substantial reductions of the Mn(II)−O hyperfine couplings. In p21·Mn(II)·GDP, for example, subtle alteration of the chemical environment of the nucleotide induced by protein mutations leads to readily observed variations in the $[\beta\text{-}^{17}O_4]$GDP hyperfine couplings (Feuerstein *et al.*, 1987).

The small ^{17}O hyperfine coupling observed in $[^{17}O_\gamma]$Thr35-labeled p21·Mn(II)·GMPPNP is certainly more similar to values observed in Mn(II) complexes with phosphate ligands than to any of the values observed with aquo ligands. In light of the greater chemical similarity of the threonine hydroxyl group to aquo rather than phosphate ligands, this result reinforces the contention that the Mn−O linkage in p21·Mn(II)·GMPPNP is strained: like the phosphate nucleotide ligands, the Mn(II)−O_γ coordination structure is influenced by the covalent bonds that link Thr35 with the rest of the protein, as well as hydrogen bonds and other noncovalent contacts with the protein, the nucleotide, and structurally-integrated solvent. Apparently, in solution, these interactions prevent Thr35 from forming a more typical bond to the Mn(II) and thus exhibiting a more typical hyperfine coupling.

MO calculations carried out on the model compound $Mn(H_2O)_6^{2+}$ indicate that this small hyperfine interaction is most probably the result of an unusually long Mn−O_γ bond[3] of ∼2.7 Å. This interpretation is in complete accord with all of the spectroscopic results. In particular, ESEEM studies of GMPPMP complexes of p21 with various isotope labels at Thr35 reveal an Mn(II)−[3-^{2}H] distance of 4.85 ± 0.2 Å (Halkides *et al.*, 1994) and a Mn(II)−[3-^{13}C] distance of 4.3 ± 0.2 Å (Farrar *et al.*, personal communication); data from

the crystal structure of threonine (Shoemaker *et al.*, 1950) imply that these two distances place absolute lower limits on the Mn(II)−oxygen bond length of 2.8 and 3.0 Å, respectively.

Functional Implications. Both Raf-1 and GAP are known to bind p21 more tightly in the GTP state than the GDP state (Moodie *et al.*, 1993; Vogel *et al.*, 1988). These results indicate that a conformational difference must exist between p21·GDP and p21·GTP when associated with these partner proteins. In light of the role of p21 as a regulatory switch, (Bourne *et al.*, 1990; Milburn *et al.*, 1990) a conformation difference must also be expected between p21·GDP and p21·GTP prior to their association with the partner proteins. Mutagenesis studies have indicated that residues in the region 26−60 are essential for p21 to bind its effectors and that residues 31−39 and 57−65 are essential for interaction with GAP and/or NF-1 (John *et al.*, 1993; Marshall, 1993; Shirouzu *et al.*, 1994; Sung *et al.*, 1995; White *et al.*, 1995). Thus, these studies suggest that residues 31−39, the Switch I region (Milburn *et al.*, 1990), are of importance in actuating the conformational change.

The presence of a nucleotide-associated conformational change in p21 involving residues 31−39 has been directly observed by X-ray crystallography (Pai *et al.*, 1990; Tong *et al.*, 1991) and by magnetic resonance spectroscopy (Halkides *et al.*, 1994; Miller *et al.*, 1993, 1992). We have emphasized that ESEEM and EPR give results that differ from those obtained by crystallography regarding metal coordination of the Thr35 hydroxyl group; it is likewise worth noting that differences exist among various X-ray structures regarding the position of Thr35 in p21 (Halkides *et al.*, 1994). Nevertheless all of the structural studies give a qualitatively similar picture of the impact of nucleotide exchange: all map a pivotal structural change in residues 30−38 that specifically positions Thr35 closer to the metal ion in the GTP form than in the GDP form of p21.

Following the crystallographic studies, the coordination of the Thr35 hydroxyl group by the divalent cation was regarded as an energetically favorable event that drives the conformational change observed in its neighborhood (Marshall, 1993; Milburn *et al.*, 1990; Pai *et al.*, 1990). Our ESEEM and EPR results clearly indicate that the metal-ligand interaction is weak and is properly regarded as incidental to the conformational change, rather than its driving force. This conclusion is reasonable strictly on energetic grounds as well. The free energy change associated with the replacement of an aquo ligand by the Thr35 hydroxyl group can be considered as the sum of local effects, characteristic of the metal oxygen binding, and nonlocal effects, which do not involve the metal−oxygen interaction. Clearly, the local effects are necessarily very similar in both the GDP and GTP forms of p21. Thus, the contrary behavior of the GDP and GTP forms of p21 as regards Mn(II)−[O_γ]Thr35 binding must be a consequence of nonlocal effects. The assumption that the metal ligand interaction is energetically dominant and thus "drives" the nucleotide-dependent conformational change, however, asserts the opposite: that the nonlocal effects are negligible. Manifestly, the decisive role in effecting the nucleotide-dependent conformational changes is played not by threonine coordination but by the other (nonlocal) interactions between the protein and the metal-nucleotide complex.

The most salient difference between the GDP and GTP forms of p21 is, obviously, the presence of the γ-phosphate in the latter, which furnishes both additional negative charge, and potential hydrogen-bonding interactions. It is tempting to suggest that the H-bond that links the γ-phosphate and Thr 35 amide group (Milburn *et al.*, 1990; Pai *et al.*, 1990) plays the primary role in driving the conformational change in the Switch I region of p21. Interestingly, another H-bond that involves the γ-phosphate, linking it to the amide group of Gly60, may likewise be largely responsible for the nucleotide-dependent conformational change in the Switch II region of p21 (Milburn *et al.*, 1990; Miller *et al.*, 1993, 1992; Sung *et al.*, 1995).

The attention focused on Thr35, together with the rigid conservation of this residue among related proteins, has motivated numerous mutagenesis studies directed at this site. Mutations affecting Thr35 may cause changes in effector binding, in GAP binding, or in GAP-dependent acceleration of GTP hyrdolysis, as has been discussed (Halkides *et al.*, 1994). The T35S mutant binds GAP and hydrolyzes GTP in GAP-dependent manner, whereas the T35A mutant loses both activities. Whether the non-transforming T35S mutant can interact with its downstream target, Raf-1, appears to depend on the particulars of the assay (Shirouzu *et al.*, 1994; White *et al.*, 1995); however, other downstream effectors can interact with the T35S mutant (White *et al.*, 1995). These data suggest that, at residue 35, a hydroxyl group is necessary, but not sufficient, to equip p21 for proper interactions with other proteins. In addition, mutation of Ser17 to Asn has been hypothesized to disrupt the coordination of Thr35 in this dominant inhibitory mutant (Farnsworth & Feig, 1991). Mutagenesis experiments, however, have not yet truly evaluated the function of the hydroxyl group at position 35, because the substitutions which have been made at this position have not merely removed or altered the position of the hydroxyl group (Ala, *allo*-Thr) but have also changed or removed the methyl group. To elucidate the role of the hydroxyl group of Thr35 while keeping the methyl group intact would require the testing of one or more of the following substitutions at this position: Val, α-aminobutyrate, or O_γ-methylthreonine.

The structural basis by which mutations within p21 disrupt interactions with other proteins is unclear. A suggestion, however, emerges from the recently reported structure of the complex between an effector of p21, Raf-RBD, and a relative of p21, Rap1A, which has a sequence identical to p21 between residues 32 and 44. While Thr35 of Rap1A is not in direct contact with Raf-RBD, its hydroxyl group is hydrogen-bonded, via a water molecule, to its Asp38, which forms a salt bridge with Arg89 of Raf-RBD (Nassar *et al.*, 1995). Removal of the hydroxyl group might enable a mispositioning of Asp38 and consequent disruption of this interprotein interaction. The loss of Raf-1 binding function in the T35S mutant may have a similar origin: removal of

[3] An alternative explanation for the small value of the experimentally determined hyperfine coupling constant is that the incorporation of isotopically labeled threonine is lower than expected. However, the enrichment is determined by GC/MS analysis of protein hydrolyzate in both the ESEEM work and the present EPR study (Figure 1). The 89% enrichment of the protein, relative to the starting amino acid, falls in the range previously observed for the enrichment of threonine residues, 75−89% (Halkides *et al.*, 1994). Thus, the level of incorporation of labeled threonine is consistently high and is explicitly taken into each analysis.

the γ-methyl group may again allow dislocation of the hydroxyl group and ultimately disrupt the interprotein salt bridge. Thus, the importance of the hydroxyl group may lie in its interactions not with the metal, but with other parts of p21. Finally, it is also worth noting that the hydrogen bond network discussed above, that links the amide groups of Thr35 and Gly60 *via* the GTP γ-phosphate, is more tightly knit in the Raf-1(RBD)−Rap1A complex than in the unassociated p21 protein (Nassar *et al.*, 1995). This comparison tends to underscore the significance of interactions involving the *amide* group of Thr35 and Gly60 and also gives some preliminary indication of potentially important conformational changes that might occur when p21 is associated with its partners.

ACKNOWLEDGMENT

We thank the following people for assistance with this work: Professor George Reed (University of Wisconsin−Madison) for determining the value of the zero-field splitting parameter of p21·Mn(II)·GMPPNP; Professor Lawrence Feig (Tufts University) for the gift of plasmid pXVR; Andrew Tyler (Harvard University) and James Evans (The Eunice K. Shriver Center) for mass spectrometric determinations and helpful discussions; Professor William Klemperer (Harvard University) for use of the *Gaussian 92* suite of programs; Souheil Inati (MIT) for work in the implementation of T_M measurements; Jeffrey Bryant for technical assistance; and Professor Alfred G. Redfield (Brandeis University) for support and many stimulating and enlightening discussions.

REFERENCES

Abragam, A., & Bleaney, B. (1970) *Electron Paramagnetic Resonance of Transition Ions*, Dover, New York.
Becerra, L. R., Gerfen, G. J., Bellew, B. F., Bryant, J. A., Hall, D. A., Inati, S. I., Weber, R. T., Un, S., Prisner, T. F., McDermott, A. E., Fishbein, K. W., Kreischer, K. E., Temkin, R. J., Singel, D. J., & Griffin, R. G. (1995) *J. Magn. Reson., Ser. A 117*, 28−40.
Bellew, B. F., Halkides, C. J., Gerfen, G. J., Griffin, R. G., & Singel, D. J. (1996) *Biochemistry 35*, 12186−12193.
Bourne, H. R., Sanders, D. A., & McCormick, F. (1990) *Nature 348*, 125−132.
Bruckner, S., Menabue, L., & Saladini, M. (1993) *Inorg. Chim. Acta 214*, 185−191.
Carrell, C. J., Carrell, H. L., Erlebacher, J., & Glusker, J. P. (1988) *J. Am. Chem. Soc. 110*, 8651−8656.
Carrell, H. L., & Glusker, J. P. (1973) *Acta Crystallogr. B29*, 638−640.
Ciunik, Z., & Glowiak, T. (1980) *Acta Crystallogr. B36*, 1212−1213.
Clegg, W., Lacy, O. M., & Straughan, B. P. (1987) *Acta Crystallogr. C43*, 794−797.
DeBeer, R., DeBoer, W., Hoff, C. A. v., & Ormondt, D. v. (1973) *Acta Crystallogr. B29*, 1473−1480.
Evans, D. A., & Weber, A. E. (1986) *J. Am. Chem. Soc. 108*, 6757.
Evans, D. A., Bartroli, J., & Shih, T. L. (1983) *J. Am. Chem. Soc. 105*, 5946.
Farnsworth, C. L., & Feig, L. A. (1991) *Mol. Cell. Biol. 11*, 4822−4829.
Feuerstein, J., Kalbitzer, H. R., John, J., Goody, R. S., & Wittinghofer, A. (1987) *Eur. J. Biochem. 162*, 49−55.
Frisch, M. J., Trucks, G. W., Head-Gordon, M., Gill, P. M. W., Wong, M. W., Foresman, J. B., Johnson, B. G., Schlegel, H. B., Robb, M. A., Replogle, E. S., Gomperts, R., Andres, J. L., Raghavachari, K., Binkley, J. S., Gonzalez, C., Martin, R. L., Fox, D. J., Defrees, D. J., Baker, J., Stewart, J. J. P., & Pople, J. A. (1992) *Gaussian 92*, Gaussian, Inc., Pittsbugh.
Gideon, P., John, J., Frech, M., Lautwein, A., Clark, R., Scheffler, J. E., & Wittinghofer, A. (1992) *Mol. Cell. Biol. 12*, 2050−2056.
Glotfelty, H. W. (1978) Ph.D. Thesis, University of Kansas.
Glusker, J. P., & Carrell, H. L. (1973) *J. Mol. Struct. 15*, 151−159.
Halkides, C. J., Farrar, C. T., Larsen, R. G., Redfield, A. G., & Singel, D. J. (1994) *Biochemistry 33*, 4019−4035.
Hay, P. J., & Wadt, W. R. (1985a) *J. Chem. Phys. 82*, 299.
Hay, P. J., & Wadt, W. R. (1985b) *J. Chem. Phys. 82*, 270−283.
Hyde, J. S., Jesmanowiscz, A., Ratke, J. J., & Antholine, W. E. (1992) *J. Magn. Reson. 96*, 1−13.
John, J., Rensland, H., Schlichting, I., Vetter, I., Borasio, G. D., Goody, R. S., & Wittinghofer, A. (1993) *J. Biol. Chem. 268*, 923−929.
Kalbitzer, H. R., Goody, R. S., & Wittinghofer, A. (1984) *Eur. J. Biochem. 141*, 591−597.
Karipides, A., & Reed, A. T. (1976) *Inorg. Chem. 15*, 44−47.
Latwesen, D. G., Poe, M., Leigh, J. S., & Reed, G. H. (1992) *Biochemistry 31*, 9608−9611.
Lenstra, A. T. H., & Dillon, J. (1983) *Bull. Soc. Chim. Belg. 92*, 257−262.
Lodato, D. T., & Reed, G. H. (1987) *Biochemistry 26*, 2243−2250.
Marshall, M. S. (1993) *Trends Biochem. Sci. 18*, 250−254.
Milburn, M., Tong, L., DeVos, A. M., Brunger, A., Yamaizumi, Z., Nishimura, S. & Kim, S.-H. (1990) *Science 247*, 939−945.
Miller, A.-F., Papastavros, M. Z., & Redfield, A. G. (1992) *Biochemistry 31*, 10208−10216.
Miller, A.-F., Halkides, C. J., & Redfield, A. G. (1993) *Biochemistry 32*, 7367−7376.
Moodie, S. A., Willumsen, B. M., Weber, M. J., & Wolfman, A. (1993) *Science 260*, 1658−1661.
Nassar, N., Horn, G., Herrmann, C., Scherer, A., McCormick, F., & Wittinghofer, A. (1995) *Nature 375*, 554−560.
Pai, E. F., Krengel, U., Petsko, G., Goody, R. S., Kabsch, W., & Wittinghofer, A. (1990) *EMBO J. 9*, 2351−2359.
Reed, G. H., & Leyh, T. S. (1980) *Biochemistry 19*, 5472−5480.
Reed, G. H., & Markham, G. D. (1984) *Biol. Magn. Reson. 6*, 73−142.
Sabat, M., Cini, R., Haromy, T., & Sundaralingam, M. (1985) *Biochemistry 24*, 7827−7833.
Sawyer, C. B. (1972) *J. Org. Chem. 37*, 4225.
Shirouzu, M., Koide, H., Fujita-Yoshigaki, J., Oshio, H., Toyama, Y., Yamasaki, K., Fuhrman, S. A., Villafranca, E., Kaziro, Y., & Yokoyama, S. (1994) *Oncogene 9*, 2153−2157.
Shoemaker, D. P., Donohue, J., Schomaker, V., & Corey, R. B. (1950) *J. Am. Chem. Soc. 72*, 2328−2349.
Sung, Y.-S., Carter, M., Zhong, J. M., & Hwang, Y.-W. (1995) *Biochemistry 34*, 3470−3477.
Tan, X., Poyner, R., Reed, G. H., & Scholes, C. P. (1993) *Biochemistry 32*, 7799−7810.
Tan, X., Bernardo, M., Thomann, H., & Scholes, C. P. (1995) *J. Chem. Phys. 102*, 2675−2689.
Tong, L., deVos, A. M., Milburn, M. V., Brunger, A., & Kim, S.-H. (1991) *J. Mol. Biol. 217*, 503−516.
Vasic, P., Prelesnik, B., Curic, M., & Herak, R. (1985) *Z. Kristallogr. 173*, 193−198.
Vogel, U. S., Dixon, R. A. F., Schaber, M. D., Diehl, R. E., Marshall, M. S., Scolnick, E. M., Sigal, I. S., & Gibbs, J. B. (1988) *Nature 335*, 90−93.
Wadt, W. R., & Hay, P. J. (1985) *J. Chem. Phys. 82*, 284.
Weber, A. E. (1987) Ph.D. Thesis, Harvard University.
White, M. A., Nicolette, C., Minden, A., Polverino, A., Aeist, L. V., Karin, M., & Wigler, M. H. (1995) *Cell 80*, 533−541.

BI9605954